

# Counter Rotating Wind Energy Generator for DC Micro Grid



*By*

Wasiullah khan

CUI/FA19-EPE-167/ATD

Naqash Mughal

CUI/FA19-EPE-149/ATD

Muhammad Shaheer Ahmad

CUI/FA19-EPE-172/ATD

BS Thesis

In

Electrical (Power) Engineering

COMSATS University Islamabad  
Abbottabad Campus-Pakistan

Spring 2023



**COMSATS University Islamabad-Abbottabad Campus**

# Counter Rotating Wind Energy Generator for DC Micro Grid

A Thesis Presented to

COMSATS University Islamabad- Abbottabad Campus

In partial fulfillment

of the requirement for the degree of

## BS Electrical (Power) Engineering

By

Wasiullah khan

CUI/FA19-EPE-167/ATD

Naqash Mughal

CUI/FA19-EPE-149/ATD

Muhammad Shaheer Ahmad

CUI/FA19-EPE-172/ATD

Spring 2023

# Counter Rotating Wind Energy Generator for DC Micro Grid

---

An Undergraduate Thesis submitted to Electrical and Computer Engineering Department as partial fulfillment of the requirement for the award of Degree of Bachelor of Science in Electrical (Power) Engineering.

| Name                   | Registration Number  |
|------------------------|----------------------|
| Wasiullah Khan         | CUI/FA19-EPE-167/ATD |
| Naqash Mughal          | CUI/FA19-EPE-149/ATD |
| Muhammad Shaheer Ahmad | CUI/FA19-EPE-172/ATD |

## **Supervisor**

Dr. Faisal Khan

Assistant Professor, Electrical and Computer Engineering

Abbottabad Campus

COMSATS University Islamabad (CUI)

Abbottabad Campus

July 2023

## Final Approval

---

This thesis titled.

# Counter Rotating Wind Energy Generator for DC Micro Grid

By

*Wasiullah khan*

*CUI/FA19-EPE-167/ATD*

*Naqash Mughal*

*CUI/FA19-EPE-149/ATD*

*Muhammad Shaheer Ahmad*

*CUI/FA19-EPE-172/ATD*

Has been approved.

For the COMSATS University Islamabad, Abbottabad Campus

Supervisor: \_\_\_\_\_

Dr. Faisal Khan, Assistant Professor

Department of Electrical and Computer Engineering Engineering/CUI, Abbottabad Campus

HOD: \_\_\_\_\_

Dr. Owais, Professor

Department of Electrical and Computer Engineering, CUI, Abbottabad Campus

## Declaration

I Wasiullah Khan (CIIT/FA19-EPE-167/ATD) and Naqash Mughal (CIIT/FA19-EPE-149/ATD) and Muhammad Shaheer Ahmad (CIIT/FA19-EPE-172/ATD) hereby declare that I have produced the work presented in this thesis, during the scheduled period of study. I also declare that I have not taken any material from any source except referred to wherever due that amount of plagiarism is within acceptable range. If a violation of HEC rules on research has occurred in this thesis, I shall be liable to punishable action under the plagiarism rules of the HEC.

Date: \_\_\_\_\_

Signature of the student:

\_\_\_\_\_  
Wasiullah khan  
CUI/FA19-EPE-167/ATD

\_\_\_\_\_  
Naqash Mughal  
CUI/FA19-EPE-149/ATD

\_\_\_\_\_  
Muhammad Shaheer Ahmad  
CUI/FA19-EPE-172/ATD

## Certificate

It is certified that Wasiullah Khan (CIIT/FA19-EPE-167/ATD), Naqash Mughal (CIIT/FA19-EPE-149/ATD) and Muhammad Shaheer Ahmad (CIIT/FA19-EPE-172/ATD) has carried out all the work related to this report under my supervision at the Department of Electrical and Computer engineering, COMSATS University Islamabad, Abbottabad Campus and the work fulfills the requirement for award of BS degree.

Date: \_\_\_\_\_

Supervisor:

\_\_\_\_\_  
Dr. Faisal Khan, Assistant Professor  
Department of Electrical and Computer Engineering  
CUI, Abbottabad Campus

Head of Department:

\_\_\_\_\_  
Dr. Owais, Professor  
Department of Electrical and Computer Engineering  
CUI, Abbottabad Campus

## ACKNOWLEDGEMENTS

Writing this thesis has been fascinating and extremely rewarding. We would like to thank several people who have contributed to this study in many ways:

First and foremost, we would like to thank Allah Almighty for giving us good health, knowledge, ability, and opportunity to undertake this research study. After Allah, we express our sincere and deepest gratitude to our supervisor, Dr. Faisal Khan, Assistant Professor Department of Electrical Engineering, COMSATS University Islamabad, Abbottabad, for his patience, motivation, enthusiasm, and immense knowledge. His guidance helped us in our research and writing of this thesis. His expertise, invaluable guidance, constant encouragement, affectionate attitude, understanding, patience and healthy criticism added to our experience. Without his continual inspiration, it would not have been possible to complete this study. Besides our advisor, we would like to thank the rest of project committee for their encouragement, insightful comments, and hard questions.

We are highly thankful to Mr. Wasiq Ullah, who is our senior, a talented researcher, and a good friend, for his time and effort in teaching us JMAG (simulation software) and helping us throughout this study. His encouragement and critical support from the first day made our research a lot easier for us. Finally, we thank our parents and family for their prayers, support, and sincere wishes for the completion of our degree.

We would also like to acknowledge the support of the **“Pakistan Engineering Council (PEC) under scheme of Final Year Design Project (FYDP)”** that funded this project. Their financial support not only facilitated data collection and analysis but also allowed for the exploration of new direction within this study. We are deeply grateful for their contribution to the successful completion of this project.

|                               |                     |
|-------------------------------|---------------------|
| <b>Wasiullah Khan</b>         | <b>FA19-EPE-167</b> |
| <b>Naqash Mughal</b>          | <b>FA19-EPE-149</b> |
| <b>Muhammad Shaheer Ahmad</b> | <b>FA19-EPE-172</b> |

## **ABSTRACT**

# **Counter Rotating Wind Energy Generator for DC Micro Grid**

This thesis presents a Counter Rotating Wind Energy Generator for DC Micro Grid in which our focus is to design a generator for wind energy conversion, firstly we designed Three-Phase Dual Stator Field Excited Flux Switching Generator (DS-FEFSG). Our focus is to attain high power and torque density, minimize copper losses and overhang effect. The maximum power attains by dual stator configuration and copper losses and overhang reduces by using concentrated or non-Overlapped winding. The DS-FEFSG are analyze on different rotor poles (8,10,14,16,20, and 22 pole), based on initial results the DS-FEFSG deterministically optimized on the 8, 10, and 14 pole for the further improvement of electromagnetic performance. After that, the results of optimized pole compared and finally we concluded that 14 Pole machine is the best candidate for the proposed wind generator. After optimization the author realized that electromagnetic performance of the DS-FEFSG is not fulfill the required objectives, so author move on hexagonal study. Hexagonal machine based on single stator and rotor, armature winding, and field excitation source are placed on the stationary part of the machine, so rotor is just like iron piece with lamination, power and torque density improved due to the hexagonal structure and overhang effect and copper losses reduces by using non-Overlapped winding.



# Table of Contents

|   |           |
|---|-----------|
| <b>Declaration.....</b>   | <b>5</b>  |
| <b>Certificate .....</b>  | <b>6</b>  |
| <b>ACKNOWLEDGEMENTS .....</b>                                   | <b>7</b>  |
| <b>ABSTRACT.....</b>  | <b>8</b>  |
| <b>Chapter 1 .....</b>  | <b>15</b> |
| <b>INTRODUCTION.....</b>  | <b>15</b> |
| 1.1 Introduction:.....  | 16        |
| 1.2 Problem Statement:.....                                     | 16        |
| 1.3 Objectives: .....   | 17        |
| 1.4 Scopes: .....   | 17        |
| <b>Chapter 2 .....</b>  | <b>18</b> |
| <b>Literature Review .....</b>                                  | <b>18</b> |
| 2.1 Introduction:.....  | 19        |
| 2.1.1 Classification of Electric Generators:.....               | 19        |
| 2.2 Synchronous Generators (SG): .....                          | 19        |
| 2.2.1 Construction of Synchronous Generator or Alternator:..... | 20        |
| 2.2.2 Working Principle of Synchronous Generator:.....          | 20        |
| 2.3 Induction Generator: .....                                  | 20        |
| 2.3.1 Working Principle of Induction Generator:.....            | 21        |
| 2.4 Flux Switching Generator:.....                              | 22        |
| 2.4.1 Flux Switching Permanent Magnet Machines (FSPM): .....    | 22        |
| 2.4.2 Field Excited Flux Switching Machines (FEFSM):.....       | 24        |
| <b>Chapter 3 .....</b>  | <b>25</b> |
| <b>Design Methodology.....</b>                                  | <b>25</b> |
| 3.1 Initial Design:.....  | 26        |
| 3.1.1 JMAG Designer: .....                                      | 26        |
| 3.1.2 Conventional Design:.....                                 | 26        |
| 3.1.3 Initial Proposed Design:.....                             | 27        |
| 3.2 JMAG Designer Software Work:.....                           | 28        |
| 3.2.1 Geometry Editor:.....                                     | 28        |

|   |           |
|---|-----------|
| 3.2.2Core Materials: .....                                    | 28        |
| 3.2.3JMAG Designer: .....                                     | 32        |
| 3.3 Mathematical Calculation: .....                           | 36        |
| 3.4 Initial Design:.....                                      | 36        |
| 3.4.1Flux Linkage: .....                                      | 37        |
| 3.4.2Cogging Torque: .....                                    | 37        |
| 3.4.3Average Torque: .....                                    | 38        |
| 3.4.4Back EMF: .....  | 38        |
| 3.4.5Comparison: .....  | 38        |
| 3.5 Optimization: .....                                       | 39        |
| 3.5.1Electromagnetic performance of Optimized Poles: .....    | 39        |
| 3.5.2Selected Pole for proposed machine: .....                | 42        |
| <b>Chapter 4 .....</b>  | <b>43</b> |
| <b>Hexagonal Machine and prototype .....</b>                  | <b>43</b> |
| 4.1 Hexagonal Machine: .....                                  | 44        |
| 4.1.1 Electromagnetic performance of hexagonal machine: ..... | 44        |
| 4.2 Prototype:.....   | 46        |
| <b>Chapter 5 .....</b>  | <b>48</b> |
| <b>Comparison of DS-FEFSG and Hexagonal Machine. ....</b>     | <b>48</b> |
| 5.1 Comparison:.....  | 49        |
| <b>Chapter 06 .....</b>                                       | <b>50</b> |
| <b>Conclusion .....</b>                                       | <b>50</b> |
| 6.1 Conclusion: .....   | 51        |
| <b>Chapter 7 .....</b>  | <b>52</b> |
| <b>References .....</b>                                       | <b>52</b> |
| 7.1 References.....   | 53        |

## LIST OF FIGURES

---

|  |    |
|--|----|
| Fig 2.1 Structure Diagram of Synchronous Generator .....                       | 20 |
| Fig 2.2 Wind Generating System for Induction Generator.....                    | 21 |
| Fig 2.3a Flux Linkages between Rotor and Stator at 4 Different Positions ..... | 23 |
| Fig 2.3b Flux Linkages and Back EMF .....                                      | 23 |
| Fig3.1 Conventional FSG machine design.....                                    | 25 |
| Fig 3.2 Conventional FSG winding arrangement.....                              | 27 |
| Fig 3.3 Initial proposed design of DS-FEFSG.....                               | 27 |
| Fig 3.4 Inner Stator.....  | 29 |
| Fig 3.5 Rotor.....   | 29 |
| Fig 3.6 Outer Stator.....  | 30 |
| Fig 3.7a Inner stator armature winding.....                                    | 30 |
| Fig 3.7b Inner stator Excitation winding.....                                  | 31 |
| Fig 3.8a Outer stator armature winding.....                                    | 31 |
| Fig 3.8b Outer stator Excitation winding.....                                  | 31 |
| Fig 3.9 Complete Model.....  | 32 |
| Fig 3.10 Material Toolbox.....   | 33 |
| Fig 3.11 Condition Toolbox.....  | 33 |
| Fig 3.12 Armature Winding Circuit.....   | 34 |
| Fig 3.13 Excitation Winding Circuit.....                                       | 34 |
| Fig 3.14 Creating Mesh.....  | 34 |
| Fig 3.15 Properties for setting end time & steps.....                          | 35 |
| Fig 3.16 Properties for setting stack length.....                              | 35 |
| Fig 3.17 Results.....  | 36 |
| Fig 3.18 Coil flux Linkage (Initially).....                                    | 37 |
| Fig 3.19 Cogging Torque (Initially).....                                       | 37 |
| Fig 3.20 Average Torque (Initially).....                                       | 38 |
| Fig 3.21 Back EMF (Initially).....   | 38 |
| Fig 3.22(a) Flux Distribution 10 pole (optimized).....                         | 40 |
| Fig3.22(b) Flux Distribution 14 pole (optimized).....                          | 40 |
| Fig3.22(c) Flux Distribution 14 pole (optimized).....                          | 40 |
| Fig 3.23 Cogging torque (optimized) .....                                      | 41 |

|   |    |
|---|----|
| Fig 3.24 Average torque (optimized).....    | 41 |
| Fig 3.25 Coil flux Linkage (optimized)..... | 41 |
| Fig 3.26 Back emf (optimized).....          | 42 |
| Fig 4.1: Design of hexagonal machine.....   | 44 |
| Fig 4.2: Cogging torque.....                | 44 |
| Fig 3.26 Back emf (optimized).....          | 45 |
| Fig 3.26 Back emf (optimized).....          | 45 |
| Fig 3.26 Back emf (optimized).....          | 45 |
| Fig 3.26 Back emf (optimized).....          | 46 |
| Fig 3.26 Back emf (optimized).....          | 46 |
| Fig 3.26 Back emf (optimized).....          | 47 |
| Fig 3.26 Back emf (optimized).....          | 47 |

## **LIST OF Tables**

---

|  |    |
|--|----|
| Table 3.1 Parameters of Proposed Design.....   | 29 |
| Table 3.2 Materials & Conditions.....  | 34 |
| Table 3.3 Comparison of Initial 8 Pole, 10 Pole, 14 Pole, 16 Pole, 20 Pole, and 22 Pole..... | 41 |
| Table 3.4 Comparison of Optimized 8 Pole, 10 Pole and 14 Pole .....                          | 44 |
| Table 4.1 Electromagnetic performance of hexagonal machine.....                              | 48 |
| Table 5.1 Comparison of DS-FEFSG and Hexagonal Machine.....                                  | 51 |

## ABBREVIATIONS

---

|         |  |
|---------|--|
| DSFSM   | Dual Stator Flux Switching Machines                |
| PMs     | Permanent Magnets                                  |
| FEFSG   | Field Excited Flux Switching Generator             |
| A.C     | Alternating Current                                |
| D.C     | Direct Current                                     |
| FE      | Field Excitation                                   |
| FEC     | Field Excitation Coil                              |
| DS      | Dual Stator  |
| DSFSG   | Dual Stator Flux Switching Generator               |
| DFIG    | Doubly Fed Induction Generator                     |
| PMSG    | Permanent Magnet Synchronous Generator             |
| FSG     | Flux Switching Generator                           |
| SG      | Synchronous Generators                             |
| FEFSM   | Field Excited Flux Switching Machines              |
| FSPM    | Flux Switching Permanent Magnet                    |
| DS-FEFS | Dual Stator Field Excited Flux Switching Generator |
| EMF     | Electro Motive Force                               |
| PM-FSG  | Permanent Magnet Flux Switching Generator          |

## **Chapter 1**

### **INTRODUCTION**

## **1.1 Introduction:**

The prospective growth in necessity and protection of the natural environment dictating global warming compels to rise the expansion of renewable energy. In the renewable energy sources wind energy is plentiful in nature, therefore expansion of wind energy ruled net renewable power generation capacity. Renewable energy resources are cost effective and viable energy resources. The DSFSG (Dual Stator Flux Switching Generator) is proposed for this type of system. Due to the high-power density and cost efficiency of field excited DS (dual stator) machines, they are widely used for domestic purposes, residential purposes, renewable energy, industrial manufacturing and many more. These machines are highly preferable due to the DC windings placed at the stator and these machines are cost effective and reliable as well.

Flux switching machines (FSMs) offer an important role in various high torque applications. In these machines, the flux sources such as field excitation coil (FEC), armature winding, and permanent magnet (PM) are in the stator while leaving the rotor part as winding less and These machines have robust mechanical structure and can rotate at high speed due to robust rotor. However, FSMs with single stator associate with limited free space for active sources in stator, which leads to some drawbacks of complicated structure, less path for flux flow, flux cancellations, heat generation and demagnetizing effects.

To overcome this issue, FSMs using double stator (DS) have been proposed. DS (Dual Stator) machines high power density, high torque density, more path for flux flow, less flux cancelation and robust structure of rotor. Dual stator machines can generate high power density and high torque density due to extra windings placement.

The proposed design is based on the dual stator flux switching generator (DSFSG), with DC excitation placed on inner and outer stator. The output is obtained by both stators and due to which the power density of this machine is increases. The overall efficiency of DSFSG is more than the conventional generators, due to power extraction from both stators. The overall cost also reduces due to the DC excitation of the generator as compared to PMs.

## **1.2 Problem Statement:**

The installed conventional generators are doubly fed induction generator (DFIG) and permanent magnet synchronous generator (PMSG).

Doubly Fed Induction Generator (DFIG) have

- Low power density



- Low efficiency
- Complex rotor
- Permanent Magnet Synchronous Generator (PMSG) have
- Rare earth materials
- Expensive due to PMs
- To overcome this problem DSFSG is proposed to obtain.
- High Power density
- High Torque Density
- Low cost due to DC windings
- Robust Mechanical Structure

In DSFSG, if the distributed windings are done, then there would be effect of overhang, more copper losses will be obtained, and the output voltage generated will be trapezoidal. So, Concentrated windings (single tooth windings) are done to obtain a sinusoidal output voltage and less copper losses. The overhang effect will also be minimized in this type of winding.

### **1.3 Objectives:**

The objectives of this project are.

- To design Dual-Stator Field Excited flux switching generator.
- To investigate the performance of machine by using concentrated windings and obtain Output Phase Voltage, Torque, Power, Coil Flux Linkage and Minimum Cogging Torque and Minimum Power Losses.
- To analyze the Dual Stator Flux Switching Generator on concentrated windings.

### **1.4 Scopes:**

- This project is designed by using JMAG Design Version 16 software.
- The FEM Coil Current,  $I_f$  is set 8A.
- The machine is operated at 1500rpm.

## **Chapter 2**

### **Literature Review**

## **2.1 Introduction:**

A Recently, concern over global warming has led to an average increase in using renewable energy sources such as wind energy, solar energy, tidal energy, etc. In the renewable energy sources wind energy is plentiful in nature, therefore expansion of wind energy ruled net renewable power generation capacity. Renewable energy resources are cost effective and viable energy resources. The worldwide total cumulative installed electricity generation capacity from wind power 733 GW, but in Pakistan it is just 1,236Megawatt. The different generators are used for wind power generation like Induction generators, synchronous generators, flux switching Generators (FSG) and many more. Among them FSG are preferable due to high power density, high efficiency, robust rotor, and compact mechanical structure.

### **2.1.1 Classification of Electric Generators:**

The generators are classified into two types.

- **DC Generators**
- **AC Generators**

There are different types of DC generators such as Permanent Magnet, Separately Excited, and Self-Excited DC generators.

There are multiple types of AC generators such as induction generators, synchronous generators, permanent magnet generators and flux switching generators (FSG).

Recently, the interest in the flux switching machine (FSM) has been increasing due to its suitability for various applications such as wind power generators, electric vehicles, electric aircraft, linear motors, and automotive applications.

Among them AC generators are discussed briefly below.

## **2.2 Synchronous Generators (SG):**

A synchronous generator is a synchronous machine which converts mechanical power into AC electric power through the process of electromagnetic induction.

Synchronous Generator, that is, an alternator (AC generator) with the same rotor speed as the rotating magnetic field of the stator. Synchronous generator is one of the most used alternators. In the modern power industry, it is widely used in hydropower, thermal power, nuclear power generation and diesel power generation.

A synchronous generator can be either single-phase or poly-phase (3phase).

## 2.2.1 Construction of Synchronous Generator or Alternator:

As alternator consists of two main parts viz.

- **Stator:** The stator is the stationary part of the alternator. It carries the armature winding in which the voltage is generated. The output of the alternator is taken from the stator.
- **Rotor:** The rotor is the rotating part of the alternator. The rotor produces the main field flux.

## 2.2.2 Working Principle of Synchronous Generator:

An alternator or synchronous generator works on the principle of electromagnetic induction, i.e., when the flux linking a conductor changes, an EMF is induced in the conductor. When the armature winding of alternator subjected to the rotating magnetic field, the voltage will be generated in the armature winding.

When the rotor field winding of the alternator is energized from the DC windings, the alternate N and S poles are developed on the rotor. When the rotor is rotated in the anticlockwise direction by a prime mover, the armature conductors placed on the stator are cut by the magnetic field of the rotor poles. As a result, the EMF is induced in the armature conductors due to electromagnetic induction. This induced EMF is alternating one because the N and S poles of the rotor pass the armature conductors alternatively. The direction of the generated EMF can be determined by the Fleming's right rule and the frequency of it is given by,

$$f = \frac{ns * p}{120}$$

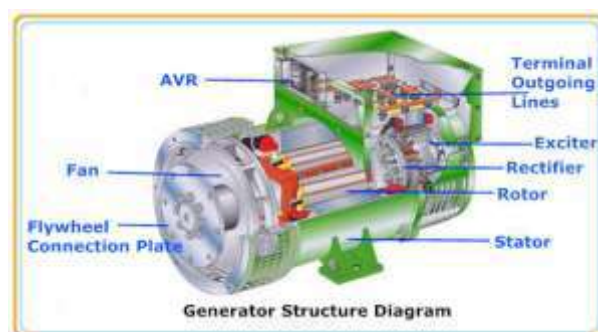


Figure 2.1: Structure Diagram of Synchronous Generator

## 2.3 Induction Generator:

Just like a DC Machine, a same induction machine can be used as an induction motor as well as an induction generator, without any internal modifications.

Induction generators are also called as asynchronous generators.

Before starting to explain how an induction (asynchronous) generator works, I assume that you know the working principle of an induction motor. In an induction motor, the rotor rotates because of slip (i.e., relative velocity between the rotating magnetic field and the rotor). Rotor tries to catch up the synchronously rotating field of the stator but never succeeds. If rotor catches up the synchronous speed, the relative velocity will be zero, and hence rotor will experience no torque.

### 2.3.1 Working Principle of Induction Generator:

Consider, an AC supply is connected to the stator terminals of an induction machine. Rotating magnetic field produced in the stator pulls the rotor to run behind it (the machine is acting as a motor). Now, if the rotor is accelerated to synchronous speed by means of a prime mover, the slip will be zero and hence the net torque will be zero. The rotor current will become zero when the rotor is running at synchronous speed.

If the rotor is made to rotate at a speed more than the synchronous speed, the slip becomes negative. A rotor current is generated in the opposite direction, due to the rotor conductors cutting stator magnetic field.

This generated rotor current produces a rotating magnetic field in the rotor which pushes (forces in opposite way) onto the stator field. This causes a stator voltage which pushes current flowing out of the stator winding against the applied voltage. Thus, the machine is now working as an induction generator (asynchronous generator).

The induction generator is not a self-excited machine. Therefore, when running as a generator, the machine takes reactive power from the AC power line and supplies active power back into the line. Reactive power is needed for producing rotating magnetic field. The active power supplied back in the line is proportional to slip above the synchronous speed.

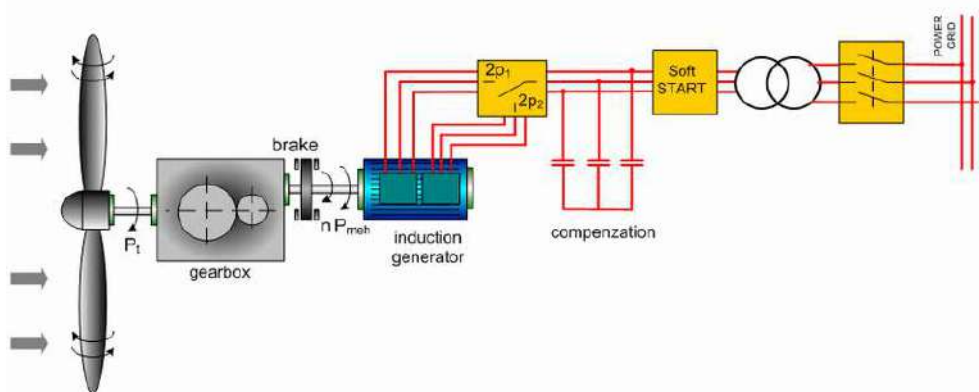


Figure 2.2: Wind Generating System for Induction Generators.

## 2.4 Flux Switching Generator:

A flux switching alternator is a form of high-speed alternator, an AC electrical generator, intended for direct drive by a turbine. They are simple in design with the rotor containing no coils or magnets, making them rugged and capable of high rotation speeds. According to the location of permanent magnets (PMs) and field excitations, these machines can be classified into two types:

- **Rotor type (RT)**
- **Stator type (ST)**

RT machines, suffer from the problem of centrifugal force in case of high-speed operation. Therefore, some appropriate measures need to be taken to hold them firmly.

As far as ST machines are concerned, the problems can be relieved since it has both the armature windings, Excitation Windings or PMs installed on the stator.

The flux Switching machines are further classified into two types, according to the excitation methods.

1. **Flux Switching Permanent Magnet Machines (FSPM)**
2. **Field Excited Flux Switching Machines (FEFSM)**

### 2.4.1 Flux Switching Permanent Magnet Machines (FSPM):

The flux-switching permanent-magnet (FSPM) machine attracts increasing attention recently due to its high-power density, robust mechanical structure, good flux-weakening capability, and essential sinusoidal back electromotive-force waveforms. Self-excited without the need for any energy source. So, it's recommended for wind turbines. The biggest plus is that it can generate power at any speed. The cost of maintenance is low. Suitable for small and light applications.

#### 2.4.4.1 Operating Principle:

The operating principle of FSPM is based on the phenomena of flux switching, which is due to facing the reluctance path and obtaining the sinusoidal flux linkage in the air gap. Let us assume a coil X, as shown in figure (a) below, when the rotor locates at position A, the rotor teeth is aligned with the stator teeth, and the magnetic resistance (reluctance) becomes the minimum. Therefore, all the magnetic flux lines go through coil X from the stator to rotor, and the PM flux linkage of coil X reaches its maximum value. Due to which flux in air gap  $\theta_r = A$ . Then, when the rotor moves to position B, the rotor teeth is aligned with the stator slots, and the magnetic resistance (reluctance) becomes the maximum. Neglecting the flux leakage, no

magnetic flux lines could go through coil X, and Due to which flux in  $\theta_r = B$ . Next, when the rotor moves to position C, the rotor teeth is aligned with the stator teeth once again, and the magnetic resistance (reluctance) becomes the minimum. Therefore, all the magnetic flux lines go through coil X from the rotor to stator, and the PM flux linkage of coil X reaches its maximum value. However, it should be noted that the direction of the magnetic flux lines going through coil X has changed compared with that in the case of position A. Therefore, the PM flux linkage of coil X is the negative maximum, which corresponds to the value of  $\theta_r = C$ . Finally, when the rotor moves to position D, the rotor teeth is aligned with two PMs. Since the permeability of PMs is equal to that of the vacuum, the magnetic resistance (reluctance) becomes the maximum once again, and no magnetic flux lines could go through coil X. This is corresponding to the value of  $\theta_r = D$ . So far, a complete period has been depicted. If the rotor continues rotating, the same process will be repeated. It can be observed from the  $\phi_{PM} - \theta_r$  curve that the PM flux linkage going through coil X varies with the relative position between the rotor teeth and the stator teeth; moreover, the polarity of PM flux linkage changes once in a cycle.

According to Faraday’s law of electromagnetic induction, the back-EMF waveform illustrated in below Fig (b) can be induced in coil X.

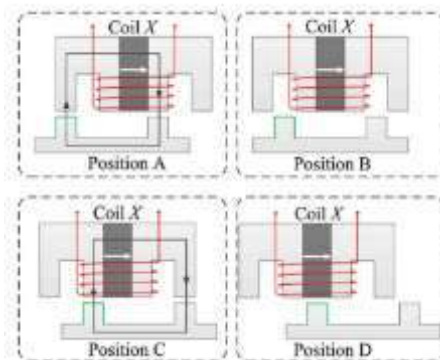


Figure 2.3(a): Flux Linkages between Rotor and Stator at 4 Different Positions

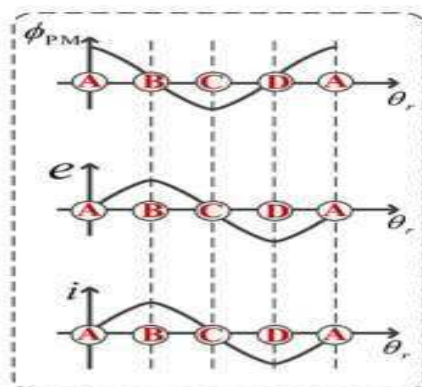


Figure 2.3(b): Flux Linkages and Back EMF

## 2.4.2 Field Excited Flux Switching Machines (FEFSM):

Although compared with permanent magnet-free (PM-free) machines the PMFS and HEFS machines have higher torque density and efficiency, the characteristics of these two kinds of flux switching machines are still compromised by the following reasons:

- The price and supply uncertainties of permanent magnets.
- The irreversible demagnetization for PMs is still possible at high temperature.
- The mechanical strength is weak for their stators, which are divided into many segments by the corresponding PMs.
- The air-gap flux density is dominated by PM excited field and the flux regulation capability is limited.

Hence, WEFS machines are proposed, where the magnets are removed, for example, PM free, and both the field and armature windings are located on the stator. Obviously, the costs of the WEFS machines are reduced and the foregoing problems concerning PMs can be easily solved in this way.

The operating principle of FEFSM is same as the operating principle of FSPM, but instead of permanent magnet, DC excitation is included, which will help to overcome the overall cost of the machine.



## **Chapter 3**

### **Design Methodology**

## 3.1 Initial Design:

### 3.1.1 JMAG Designer:

In this project, Dual Stator Field Excited Flux Switching Generator (DS-FEFSG) for wind turbine application is designed by using JMAG Designer Version 16. This software is released by Japan research institute is a FEA tool used for electromagnetic simulations. The project implementation is divided into two parts that are Geometry Editor and JMAG Designer. Geometry editor is used to design each part of machine separately such as rotor, stator, FEM-coil, field windings and armature windings while the condition setting, and simulation are developed by using JMAG Designer. JMAG is simulation software for development and design of electrical devices and drive motors for electric vehicles. The initial generator configuration and dimensions are illustrated in Figure 3.3 and Table 3.1, respectively.

### 3.1.2 Conventional Design:

As shown in Figure 3.1 (a) and (b), the conventional generator can be regarded as an integration of an inner-rotor FSG and outer-rotor FSG sharing the same stator yoke. There are two sets of windings embedded in the stator, namely the field and armature windings. The dc-field windings are toroidally wound on the stator yoke with alternating polarities in a way to imitate the PM- FSG configuration; thus, providing the same switching flux-linkage pattern. The armature windings have two winding groups, both groups are toroidally wound on the stator inward and outward teeth. The three phases of the inner armature group are connected in series with their counterparts in the outer armature group. As for the rotor, it consists of an inner rotor and outer rotor which are mechanically coupled by a disc from one end.

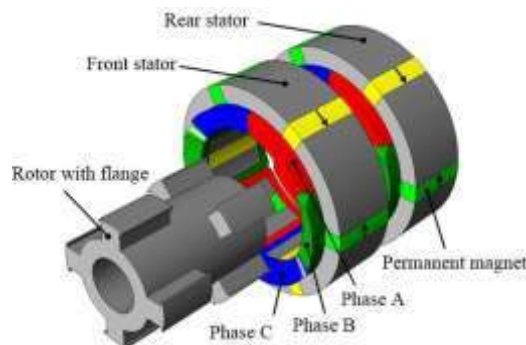


Figure 3.1: Conventional FSG Machine Design

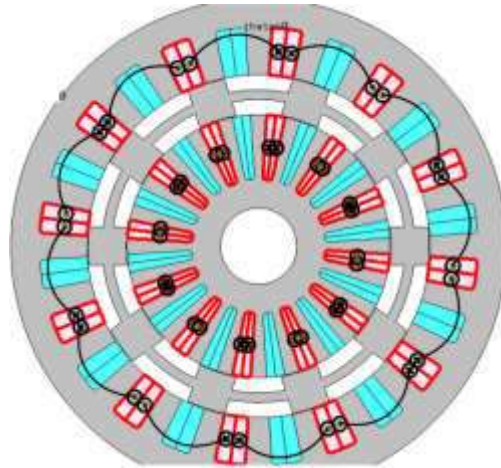


Figure 3.2: Conventional FSG Windings Arrangement

### 3.1.3 Initial Proposed Design:

The proposed DS-FEFSG contains two stators (inner and outer stator) to attain high power and torque density. There are two sets of windings embedded in the inner and outer stator, namely the field and armature windings. The concentrated (single tooth) sort of winding is used; thus, providing the same switching flux-linkage pattern. The three phases of the inner stator are connected in series with their counterparts in the outer stator. As for the rotor, it is robust in nature so we can run the proposed generator at very high speed. The proposed machine is shown in figure 3.4.

It is to be noted that in the proposed design, there is an airgap on either side of the rotor making the effective airgap. The air gap is about 0.5mm from either side of rotor so easily flux travels from stator tooth to rotor pole and complete the Path easily. The parameters of the proposed wind generator are given in Table 3.1.

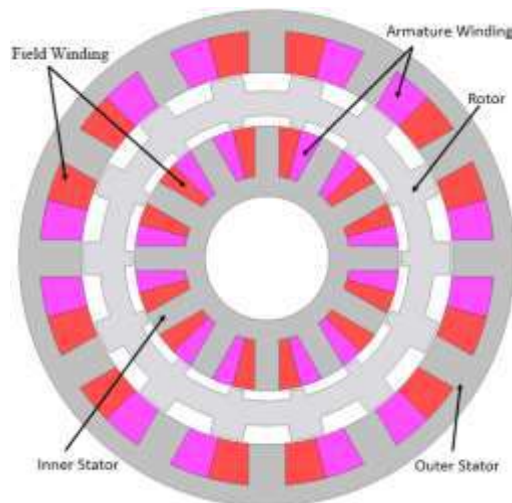


Figure 3.3: Initial Proposed Design of DS-FEFSG

Table 3.1: Parameter of Proposed Design.

| Parameters                | Value  |
|---------------------------|--------|
| Inner stator diameter     | 64 mm  |
| Outer stator diameter     | 120 mm |
| Rotor diameter            | 85 mm  |
| Shaft diameter            | 30 mm  |
| Airgap length             | 0.5 mm |
| Inner stator tooth height | 12 mm  |
| Outer stator tooth height | 10 mm  |
| Outer stator tooth width  | 9mm    |
| Inner stator tooth width  | 6mm    |
| Rotor outer pole width    | 9mm    |
| Stack length              | 50mm   |

### 3.2 JMAG Designer Software Work:

The working procedure of this software is divided into two parts,

1. Geometry Editor
2. JMAG Designer

#### 3.2.1 Geometry Editor:

Geometry Editor is used to design the machine parts such as rotor, stator, slots for AC and DC windings (field and Armature for both inner and outer stator).

The design requirements, restriction is for proposed design of dual stator flux switching generator (DS-FEFSG) for a 14 pole and 24 slots design. The restrictions for DC excitation are about 8A current.

#### 3.2.2 Core Materials:

First, the geometry of the inner stator has been designed, which is shown below in figure.

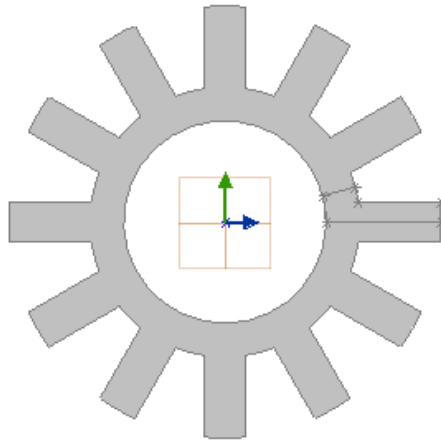


Figure 3.4: Inner Stator

The cores of the generator like inner stator, outer stator and rotor are given the same colors as grey and the excitation windings are having red color for armature windings and magenta color for excitation windings, to differentiate between the parts during assigning material in the JMAG designer.

The next part of DS-FEFSG is rotor, which is made up of steel as both stators and the rotors are the integration of outer DS-FEFSG rotor and inner DS-FEFSG rotor as shown in the figure below.

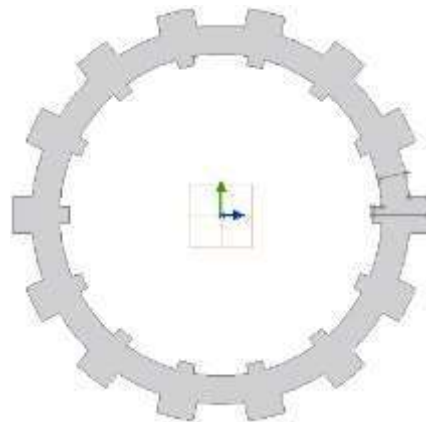


Figure 3.5: Rotor

Then comes the outer stator of the proposed design which is also made up of Nippon steel 35H210. The outer stator has outer armature and excitation windings as shown in the figure below.

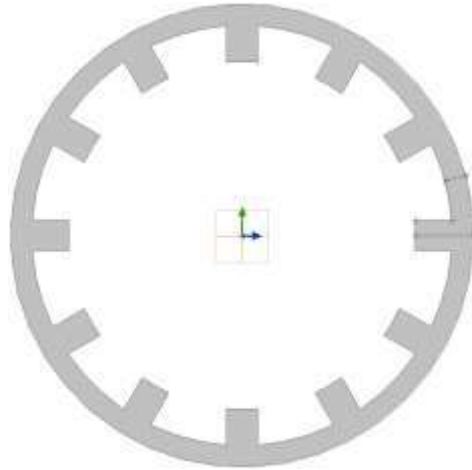


Figure 3.6: Outer Stator

### 3.2.2.1 Inner Armature and Excitation Windings:

There are two sets of windings which are embedded on the outer stator and inner stator as well namely armature windings and excitation field windings. Both the windings are concentrated windings of inner and outer stator. The connection of outer stator windings and outer stator windings is done back-to-back, which means the combination of cross dot is reversed in case of outer stator windings as compared to inner stator windings.

The inner stator windings are shown below in the figure. The magenta color is for armature windings and red color is for field excitation windings for differentiation while conditioning.

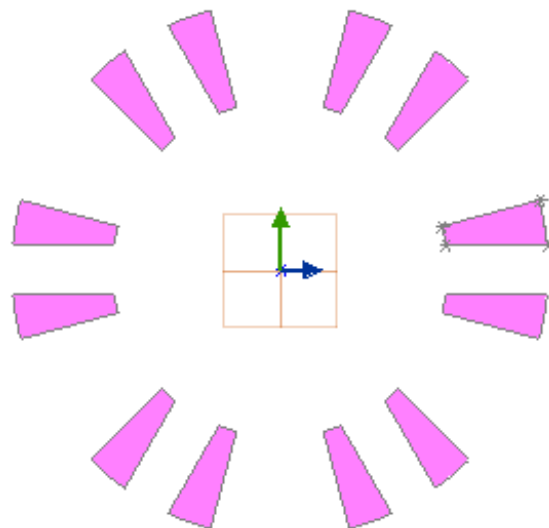


Figure 3.7(a): Inner Stator Armature winding

After that the excitation windings of inner stator comes, which are also connected in a concentrated way, or these windings are known as concentrated windings. The excitation windings are shown in figure 3.7 (b).

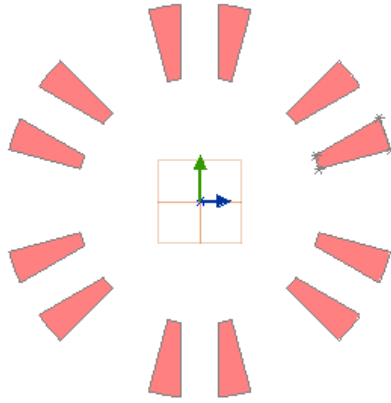


Figure 3.7(b): Inner Stator Excitation winding

### 3.2.2.2 Outer Armature and Excitation Windings:

Now here comes the outer stator armature and excitation windings of the proposed DS-FEFSG, which are also connected in a concentrated way. The connection between outer stator windings (armature and excitation) is done back-to-back with inner stator windings (armature and excitation).

The outer stator armature windings are shown in figure 3.8 (a).

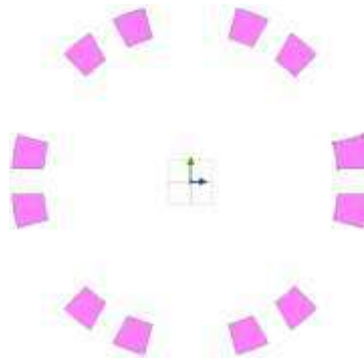


Figure 3.8(a): Outer Stator Armature Windings

Now the excitation windings or outer stator of proposed model is shown in figure 3.8 (b).

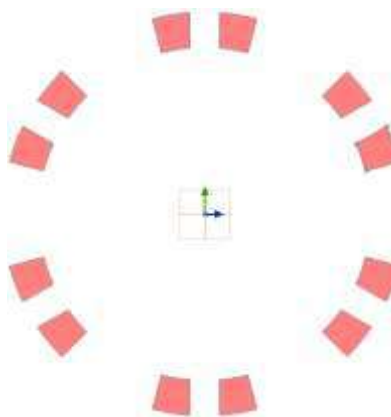


Figure 3.8(b): Outer Stator Excitation Winding

Table 3.2: Materials and Conditions

| Parts                 | Materials           | Condition                                   |
|-----------------------|---------------------|---|
| Rotor                 | Nippon Steel 35H210 | Motion: rotation<br><br>Torque: nodal force |
| Stator                | Nippon Steel 35H210 | _____                                       |
| Armature Coil         | Conductor Copper    | FEM Coil                                    |
| Excitation Field Coil | Conductor Copper    | FEM Coil                                    |

**3.2.2.3 Complete Model:**

Following the above steps for individual parts, the complete geometry in figure 3.9 is obtained.

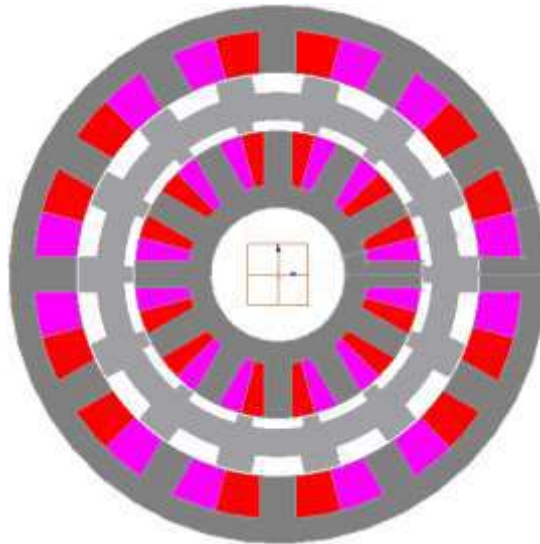


Figure 3.9: Complete Model

**3.2.3 JMAG Designer:**

JMAG Designer is used to set the machine's circuit, study properties, mesh setting, materials, and other parameters. Update this model in the JMAG Designer after creating the machine's geometry. where we conduct our magnetic transient analysis, the study's creation.

**3.2.3.1 Material Assigning:**

The next step is to choose magnetic, transient analysis to create a new study. Each component of the motor that was created in the geometry editor has its materials set. Figure



3.10 illustrates how to set the materials by clicking on the appropriate item in the toolbox on the right-hand side. Dragging the materials into each component of the motor assigns the materials.



Figure 3.10: Material toolbox

### 3.2.3.2 Conditioning:

The conditions are set by clicking the condition on toolbox, as shown in figure 3.11. Each condition is dragged into the corresponding parts.

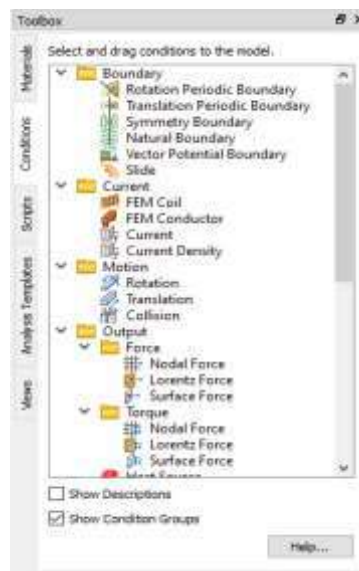


Figure 3.11: Condition Toolbox

### 3.2.3.3 Winding Circuit:

The circuit is constructed to be linked with the armature coil. Choose FEM coil in circuit toolbar and connect with the ground. Linked all armature coils with the corresponding as shown in figure 3.12.

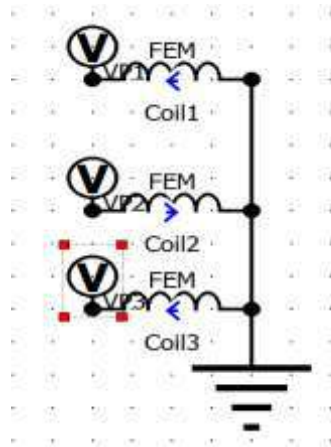


Figure 3.12: Armature winding Circuit

A different circuit is built and connected to the dc field winding coil. In the circuit toolbar, select the FEM coil, then connect it to the ground. connected to the corresponding Excitation winding coil.

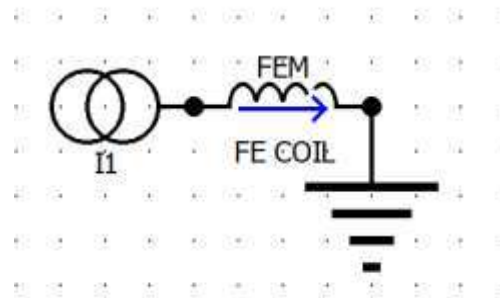


Figure 3.13: Excitation winding circuit

### 3.2.3.4 Mesh Creation and Simulation Starting:

Build the mesh. Right-click the mesh in the project manager toolbar, select Add Size Control, Part, Select All, and then click OK. Select the slide mesh option under properties, then click generate. As depicted in the figure below.

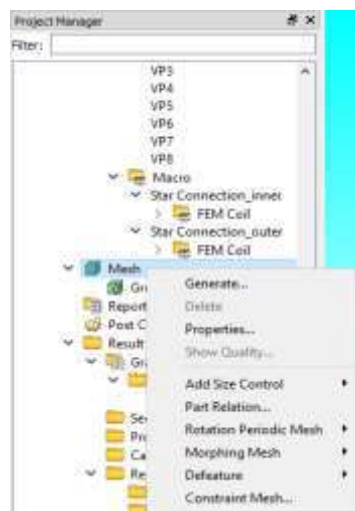


Figure 3.14: Creating Mesh

Set the magnetic properties and study. Click on study, properties, and magnetic transient. As shown in figures 3.15 and 3.16, respectively, click the step control to set the steps, end time, and division, and click the full model conversion to set the stack length.

The file is saved, and the motor is examined. Click run active case on the study toolbar. Hold off until the simulation is over. Check the outcome, then select Magnetic Flux of FEM Coil from the graph's context menu. Create the graph in Excel, then examine the results.

And then draw the circuit (coils, grouping, and power source) and connect it to the winding that you previously created in the geometry editor. Then, as shown in figure 3.17, we set additional parameters for the FEA Analysis, such as step size, end time, and mesh size.



Figure 3.15: Properties for setting End time and steps.



Figure 3.16: Properties for setting Stack length.

### 3.2.3.5 Results:

After running the simulation, results can be seen in the result section as shown in figure 3.18.

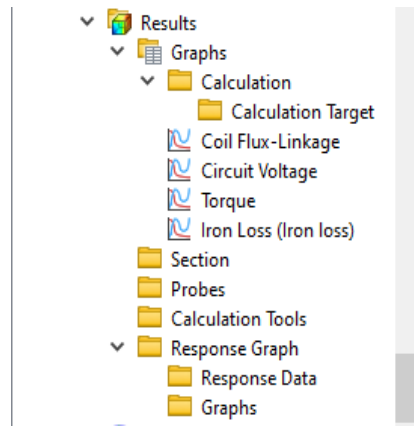


Figure 3.17: Results

### 3.3 Mathematical Calculation:

By using this formula, we calculated the electromagnetic performance of the proposed machine.

- |   |   |
|---|---|
| ➤ $p = \tau\omega$  | $Ist = \text{stacklength}$                |
| ➤ $pcus = \frac{3}{2}I^2R$  | $Cw = \text{Core Winding}$                |
| ➤ $Pcuf = I^2Rf$  | $Ww = \text{Winding Weight}$              |
| ➤ $Rf = \frac{2qN^2P'Ist}{s}$   | $Cv = \text{Core Volume}$                 |
| ➤ $Pcus = 3I^2Rs$   | $Wv = \text{Winding Volume}$              |
| ➤ $Rs = \frac{2qN^2P'Ist}{s}$   | $Rf = \text{Field Winding Resistance}$    |
| ➤ $\text{power density} = \frac{\text{total power}}{\text{total weight}}$ | $q = \text{Number of phases}$             |
| ➤ $\text{torque density} = \frac{\text{avg torque}}{\text{total weight}}$ | $N = \text{Number of turns}$              |
| ➤ $\text{total weight} = Cw + Ww$   | $P' = \text{Resistivity of Copper}$       |
| ➤ $\text{core weight} = Cv * Ist$   | $S = \text{Stack length}$                 |
| ➤ $\text{winding weight} = Wv * Ist$                                      | $Rs = \text{Resistance of Copper windig}$ |
|   | $Pcus = \text{armature copper losses}$    |
|   | $Pcuf = \text{Field copper losses}$       |
|   | $P' = \text{Resistivity of Copper}$       |
|   | $S = \text{Stack length}$                 |

### 3.4 Initial Design:

Initially the pole study of different poles like 5 to 20 has been done. In which the poles selected were those, which have 3-phase flux linkages and unipolar torque. The flux linkages at no load condition of some poles were disturbed. So, those were also rejected. The initial design has somehow sinusoidal flux linkages and unipolar average torque, like 8-pole, 10-pole, 14-pole, 16-pole, 20-pole, and 22-pole.

The comparison of these pole study has been done, where flux linkages, cogging torque, average torque has been checked initially and then among them selected poles will be optimized.

### 3.4.1 Flux Linkage:

The flux linkages of 8-pole, 10-pole, 14-pole, 16-pole, 20-pole, and 22-pole has been compared. Among them the flux linkage of 10-pole and 14-pole is better than other poles, as there is less no of harmonics in them, and the peak-to-peak value of flux linkage is better than other pole results.

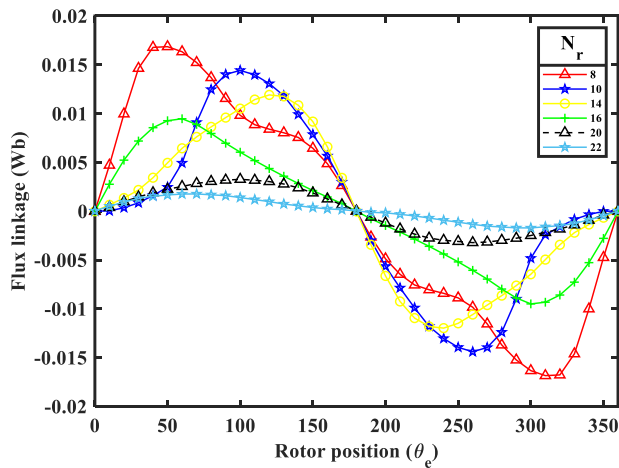


Figure 3.18: Coil Flux Linkage (Initially)

### 3.4.2 Cogging Torque:

The cogging torque of all these poles has also been considered and compared. The peak-to-peak cogging torque of every design must be less and by comparing results the 10-pole and 14-pole have peak-to-peak cogging torque less as compared to other pole designs.

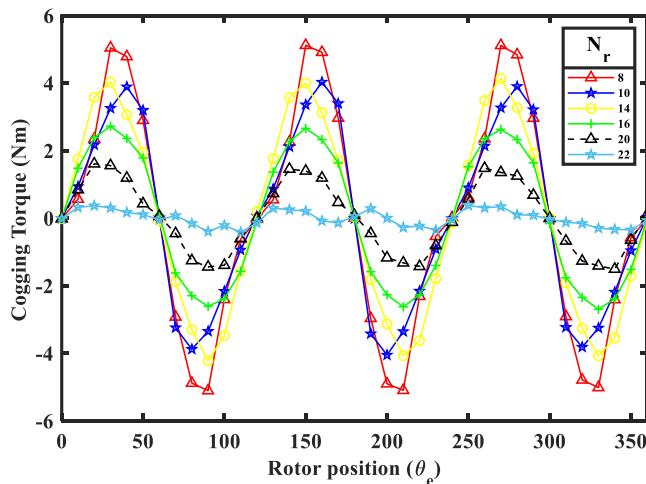


Figure 3.19: Cogging Torque

### 3.4.3 Average Torque:

At last, the average torque of each selected initial design has been checked. The average torque must be high/maximum while selecting the design. All the poles study average torque was checked and compared. The selected poles must have high average torque and 10-pole and 14-pole study have high average torque.

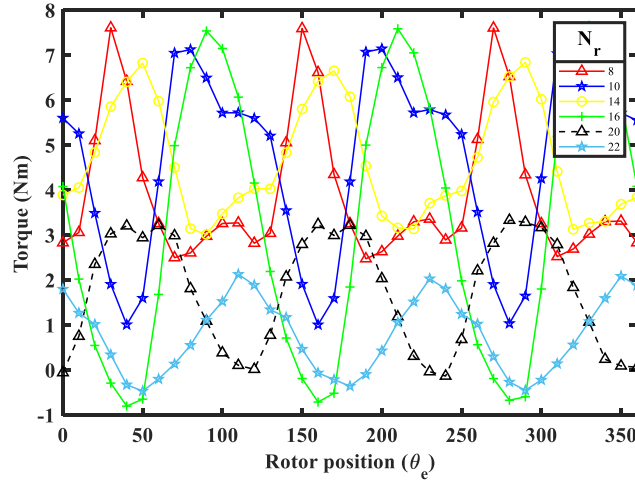


Figure 3.20: Average Torque (Initially)

### 3.4.4 Back EMF:

The back EMF of all the selected designs is shown below in the figure. As the graph shows the rich harmonics are present so we can reduce it with further optimization.

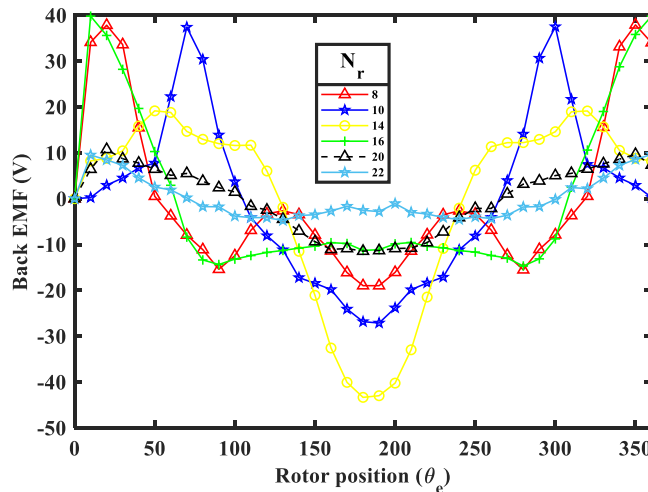


Figure 3.21: Back EMF(Initially)

### 3.4.5 Comparison:

By comparing the average torque, cogging torque, and flux linkages of all the selected designs, like 8, 10, 14, 16, 20 and 22. By comparison, the average torque of 8-pole, 10-

pole and 14-pole is higher among the others and these designs have higher flux linkages. The cogging torque of 20 and 22 poles is less, but their average torque and flux linkages are very low. So, these two poles' studies cannot be selected. The 16-pole study also has low flux linkage, low average torque, so this also cannot be selected for further optimization. For further optimization, the selected designs would be 8-pole, 10-pole, and 14-pole.

**Table 3.3: Comparison of initial 8 Pole, 10 Pole, 14 Pole, 16 Pole, 20 Pole, and 22 Pole**

| <b>S. No.</b> | <b>Pole</b> | <b>Flux linkage (p-p)</b> | <b>Cogging Torque (p-p)</b> | <b>Average Torque</b> |
|---------------|-------------|---------------------------|-----------------------------|-----------------------|
| 1             | 8           | 0.034Wb                   | 11Nm                        | 4.0039Nm              |
| 2             | 10          | 0.03Wb                    | 9.8Nm                       | 4.8534Nm              |
| 3             | 14          | 0.02Wb                    | 7.7844Nm                    | 4.0421Nm              |
| 4             | 16          | 0.018Wb                   | 8.38Nm                      | 3.10521Nm             |
| 5             | 20          | 0.008Wb                   | 4.8Nm                       | 1.8321Nm              |
| 6             | 22          | 0.005Wb                   | 2.3Nm                       | 1.5457Nm              |

### **3.5 Optimization:**

By comparing all the selected designs at the initial stage, the designs selected for further optimization were 8-pole, 10-pole and 14-pole machines were optimized. Using deterministic optimization approach, only selected parameters on the rotor were varied without changing the design parameters on the stator.

The obtained optimal results, in terms of design parameters and electromagnetic performance, are presented.

#### **3.5.1 Electromagnetic performance of Optimized Poles:**

##### **3.5.1.1 On Load Flux Density:**

The on-load flux density maps of the optimal machines are also compared in the figs below. The maximum value of the flux density is about 6% lower in the 14-pole machine compared to the 10-pole machine, which is an indication of reduced iron losses and improved efficiency in the former.

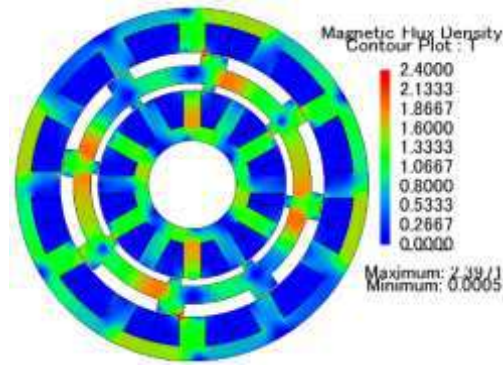


Figure 3.22(a): Flux Distribution 8-Pole (Optimized)

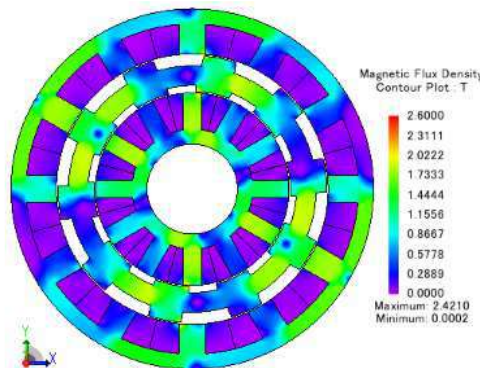


Figure 3.23(b): Flux Distribution 10-Pole (Optimized)

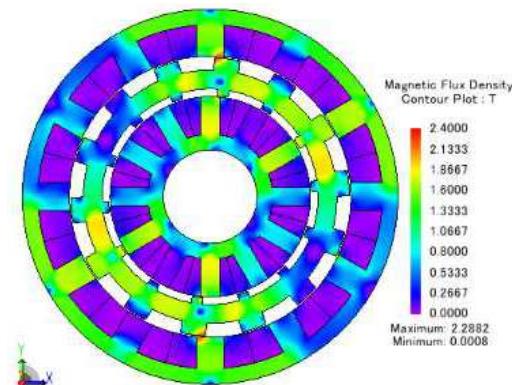


Figure 3.22(c): Flux Distribution 14-Pole (Optimized)

### 3.5.1.2 Cogging Torque:

After optimization, the peak-to-peak cogging torque of 14-pole machine reduced to 87.5% and the cogging torque of 10-pole is decreased by 78.48, and cogging torque of 8-pole is decreased by 89.5% while comparing it with the initial design. The cogging torque of 8 pole, 10 pole and 14 pole design is shown below.



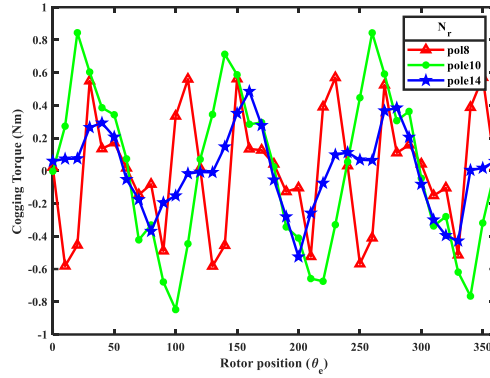


Figure 3.23: Cogging Torque (Optimized)

### 3.5.1.3 Average Torque:

The average torque of 14-pole is increased by 79.13%, the average torque of 10-pole is increased by 58.48% and the average torque of 8-pole is increased just by 3.15% as compared to initial design of both design by using deterministic approach.

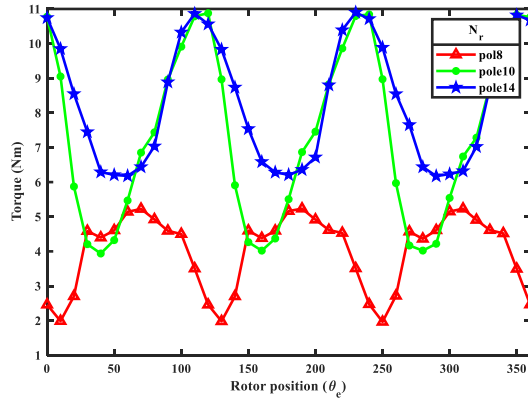


Figure 3.24: Average Torque (Optimized)

### 3.5.1.3 Flux Linkage:

For 14-pole the peak-to-peak flux linkage increased by about 53.33%, for 10-pole, the peak-to-peak flux linkage increased by 59.72% and while for 8-pole, the peak-to-peak flux linkage is decreased by 6% as compared to initial design by doing further optimization.

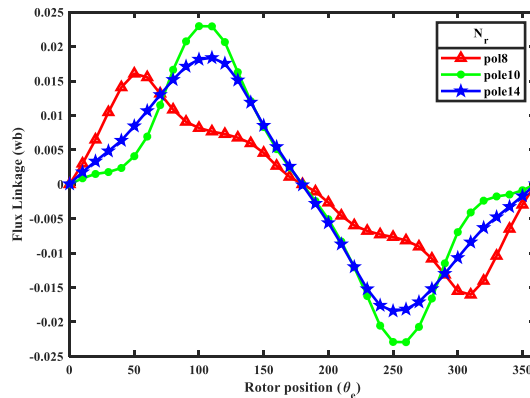


Figure 3.25: Coil Flux Linkage (Optimized)

### 3.5.1.4 Back EMF:

The back EMF of both the designs 8-pole, 10-pole and 14-pole is shown below in the graph.

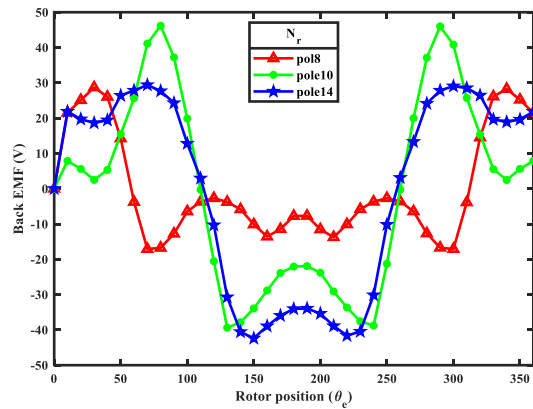


Figure 3.26: Back EMF (Optimized)

### 3.5.1.5 Comparison between optimized Pole:

By comparing 8-pole, 10-pole, and 14-poles, it is determined that the average torque and flux linkage of 8-pole study is not increased according to the constraint. While cogging torque decreased by 89.5%. The 10-pole average torque increased by 58.48%, the flux linkage increased by 59.72% and cogging torque decreased by 78.48%. The 14-pole average torque increased by 79.13%, the flux linkage increased by 53.33% and cogging torque decreased by 87.5%. All the compared results are shown Table 3.4.

Table 3.4: Comparison of optimized 8 Pole, 10 Pole and 14 Pole

| Parameters           | 8 Pole       | 10 Pole     | 14 Pole     |
|----------------------|--------------|-------------|-------------|
| Cogging Torque (p-p) | 1.153 Nm     | 1.68 Nm     | 1.015 Nm    |
| Average Torque       | 4.0538 Nm    | 7.29 Nm     | 8.24071 Nm  |
| Flux linkage (p-p)   | 0.032 Wb     | 0.046 Wb    | 0.0368 Wb   |
| Output power         | 636.44 W     | 1114.53 W   | 1293.791 W  |
| Power losses         | 407.38 W     | 450.862 W   | 538.807 W   |
| Efficiency           | 61 %         | 71.73 %     | 70.59 %     |
| Power density        | 183.322 W/Kg | 361.82 W/Kg | 419.11 W/Kg |
| Torque density       | 1.1676 Nm/Kg | 2.3 Nm/Kg   | 2.669 Nm/Kg |

### 3.5.2 Selected Pole for proposed machine:

From the comparisons of optimized pole that are given in Table 3.4, we concluded that 14 Pole machine has the optimal performance compared to other poles, the cogging torque is minimum while the average torque is high. To this end, the output power is maximum while harmonics of the flux linkage and torque ripple is decreased drastically as compared to other poles. So, the 14-Pole machine is the best candidate for the proposed wind generator.

## **Chapter 4**

### **Hexagonal Machine and prototype**

## 4.1 Hexagonal Machine:

The proposed hexagonal machine contains single rotor and stator with permanent magnet. Both armature winding and excitation source are placed on the stator. So, the rotor is simple and robust so we can run a machine at high speed and the cooling procedure quite easy for the permanent magnet due to their placement. The advantage of hexagonal machine is high power density and torque density because consumption of material is less compared to circular machine. Hexagonal machine (12slot/10pole) are shown in Figure 4.1

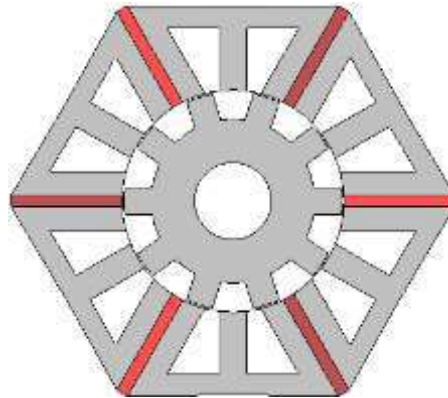


Figure 4.1: Design of hexagonal machine

### 4.1.1 Electromagnetic performance of hexagonal machine:

Electromagnetic performance of hexagonal machine in terms of Cogging torque, Flux linkage, Back-emf and average torque are discussed in this section.

#### 4.1.1.1 Cogging torque:

Cogging torque is undesirable in electric machine because it produces noise and vibration. Our objective is to minimize the cogging torque as possible. In this machine, peak-to-peak cogging torque is about 0.2Nm shown in figure 4.2.

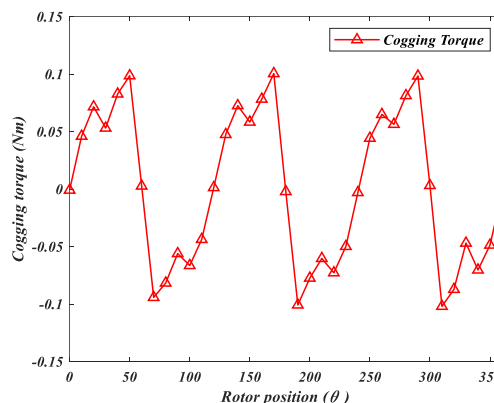


Figure 4.2: Cogging torque

#### 4.1.1.2 Average torque:

The waveform of the average torque is shown in figure 4.3, the average torque is about 5.76Nm achieved.

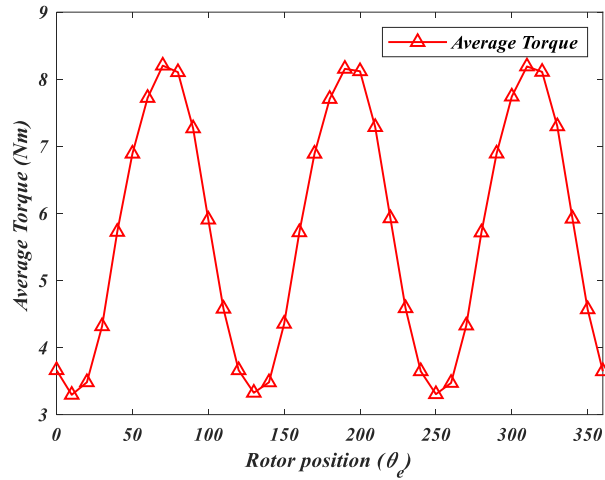


Figure 4.3: Average Torque

#### 4.1.1.3 Flux linkage:

The peak-to-peak flux linkage are shown in figure 4.4, as the waveform shows that the flux linkage is pure sinusoidal. The peak-to-peak flux linkage about 0.068Wb is attained in hexagonal machine.

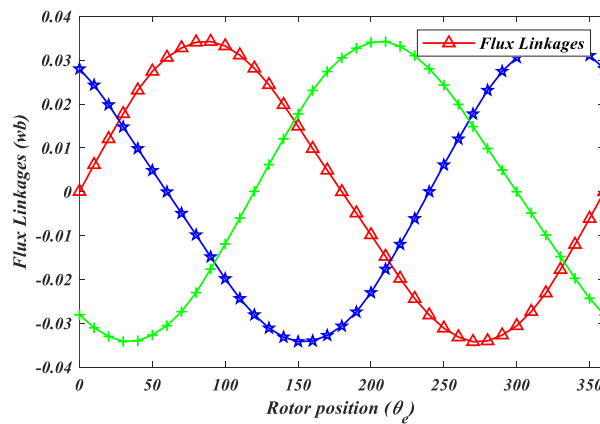


Figure 4.4: 3 phase flux linkages.

#### 4.1.1.4 Back-EMF:

The back-emf of the hexagonal machine is shown in figure 4.5. As the graph shows, the few harmonics are present in the back-emf so we can reduce these harmonics by some techniques.

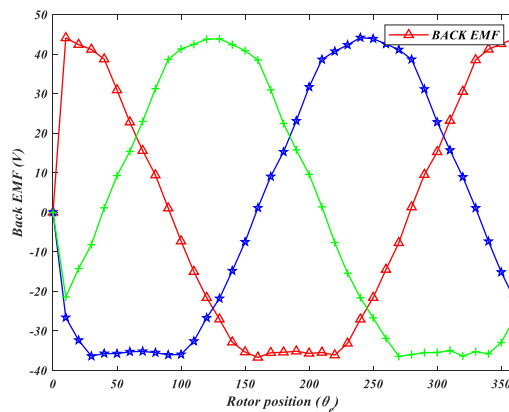


Figure 4.5: Back-EMF.

The electromagnetic performance of a hexagonal machine is also given in Table 4.1, which shows output power about 1K watt and efficiency is 91.22%.

**Table 4.1: Electromagnetic performance of hexagonal machine.**

| Electromagnetic performance | Hexagonal machine |
|-----------------------------|-------------------|
| Cogging Torque (Nm)         | 0.2               |
| Flux linkage (wb)           | 0.068             |
| Average torque (Nm)         | 5.76              |
| Output Power (watt)         | 1K                |
| Efficiency (%)              | 91.22             |
| Torque Ripples (%)          | 0.85              |

## 4.2 Prototype:

After simulation, the prototype is developed to validate the results. The internal view of the stator (12slots) is shown in Figure 4.6 and 4.7, the concentrated sort of winding is used in the proposed machine to reduces the consumption of copper losses which results, copper losses reduce. Due to the hexagonal shape of the stator the weight of the machine reduces.



**Figure 4.6: Internal view of stator.**



**Figure 4.7: Internal view of the hexagonal machine**

The final prototype with housing is shown in Figure 4.9. To check that coils are connected in correct pattern is shown in Figure 4.9



Figure:4.8 Final prototype of hexagonal machine.

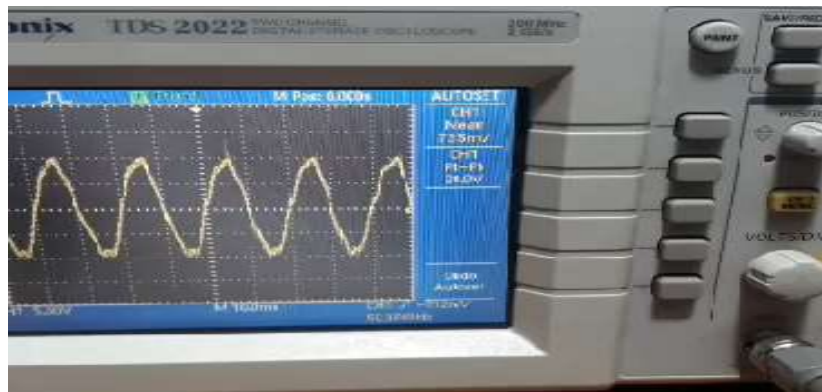


Figure:4.9: Final prototype of hexagonal machine.

## **Chapter 5**

### **Comparison of DS-FEFSG and Hexagonal Machine.**



## 5.1 Comparison:

In this section we compare both DS-FEFSG and hexagonal machine. Both machines are compared in Table 5.1, The cogging of the hexagonal machine improved about 80.29% and efficiency also improved about 22.44%. Peak-to-peak flux linkage of a DS-FEFSG have rich harmonics compared to hexagonal machine on the other hand the behavior of coil flux linkage is sinusoidal compared to the DS-FEFSG So, from this comparison we concluded that hexagonal machine is best candidate for the wind generator.

Table 5.1: Comparison of DS-FEFSG and Hexagonal Machine.

| Electromagnetic Performance | DS-FEFSG | Hexagonal Machine |
|-----------------------------|----------|-------------------|
| Cogging Torque (p-p) (Nm)   | 1.015    | 0.2               |
| Average Torque (Nm)         | 8.24     | 5.76              |
| Flux Linkage (p-p) (Wb)     | 0.036    | 0.068             |
| Output Power (watt)         | 1294     | 1K                |
| Efficiency (%)              | 70.59    | 91.22             |

## **Chapter 06**

### **Conclusion**

## 6.1 Conclusion:

In this thesis, a low-cost DS-FEFSG is proposed in which the concentrated non-overlap winding is used that reduces the copper losses, overhang effect and overall cost of the machine, the power and torque density improved due to inner and outer stator. Due to the existence of field excitation excellent flux regulation capabilities are achieved. The proposed machine is analyzed on different rotor poles (8,10,14,16,20,22) to predict the electromagnetic performance in terms of cogging torque, flux linkage, back-EMF, and electromagnetic torque profiles. The initial results show the 14-rotor pole with the highest torque at 4.65 Nm followed by 10-rotor pole machine at 4.60 Nm, with both machines also displaying least torque ripple performance. To achieve the optimal result, the 10 and 14 pole machines are then optimized and further compared. After optimization, the 14-pole machine still yields 13% higher torque at 8.24 Nm and about 40% lower torque ripple at 0.568% compared to the 10-pole machine: thus, positioning the former as the best machine for the proposed wind generator but the results of the DS-FEFSG are not quite good efficiency is low, rich harmonics are present in flux linkage and Back-emf so to obtain the required objectives we shift on the hexagonal study where we achieved almost 92% efficiency and sinusoidal flux linkage by comparing results of hexagonal machine with DS-FEFSG we concluded that Hexagonal machine is the best candidate for wind generator application.

## **Chapter 7**

## **References**

## 7.1 References

- [1] Owusu, P.A. and Asumadu-Sarkodie, S., 2016. A review of renewable energy sources, sustainability issues and climate change mitigation. *Cogent Engineering*, 3(1), p.1167990.
- [2] Ullah, W., Khan, F., Akuru, U.B., Hussain, S., Yousuf, M. and Akbar, S., "Design of a Low-Cost Dual Rotor Field Excited Flux Switching Generator for Wind Turbine Applications," *International Conference on Electrical Machines (ICEM)*, Valencia, Spain, 2022, pp. 996-1002
- [3] Yazdanpanah, R., Afroozeh, A. and Eslami, M., 2022. Analytical design of a radial-flux PM generator for direct-drive wind turbine renewable energy application. *Energy Reports*, 8, pp.3011-3017.
- [4] Khan, F., Sulaiman, E. and Ahmad, M.Z., "Coil test analysis of Wound-field three-phase flux switching machine with non-overlapping winding and salient rotor," *IEEE 8th International Power Engineering and Optimization Conference (PEOCO2014)*, Langkawi, Malaysia, 2014, pp. 243-247
- [5] Ullah, W., Khan, F., Hussain, S. and Alturise, F., 2022. Investigation of low-cost dual port co-rotating dual rotor field excited flux switching generator for low-power rooftop wind turbine integrated with multi-port DC micro grid. *IET Renewable Power Generation*, 16(14), pp.3108-3118.
- [6] Wang, P., Hua, W., Zhang, G., Wang, B. and Cheng, M., 2021. Principle of flux-switching PM machine by magnetic field modulation theory part II: Electromagnetic torque generation. *IEEE Transactions on Industrial Electronics*, 69(3), pp.2437-2446.
- [7] Meeker, D.C. and America, Q.N., 2014, May. Doubly salient synchronous generator for gas turbine engines. In *Electric Machines Technology Symp.(EMTS 2014)* (pp. 28-29).
- [8] More, D.S., Kalluru, H. and Fernandes, B.G., 2008, October. Outer rotor flux reversal machine for rooftop wind generator. In *2008 IEEE Industry Applications Society Annual Meeting* (pp. 1-6). IEEE.
- [9] Jian, L., Chau, K.T. and Jiang, J.Z., 2009. A magnetic-g geared outer-rotor permanent-magnet brushless machine for wind power generation. *IEEE Transactions on Industry Applications*, 45(3), pp.954-962.

- [10] Yu, C., Chau, K.T. and Jiang, J.Z., 2009. A flux-mnemonic permanent magnet brushless machine for wind power generation. *Journal of applied Physics*, 105(7), p.07F114.
- [11] Fan, Y., Chau, K.T. and Cheng, M., 2006. A new three-phase doubly salient permanent magnet machine for wind power generation. *IEEE Transactions on Industry Applications*, 42(1), pp.53-60.
- [12] Ullah, W. and Khan, F., 2021. Design and performance analysis of a novel outer-rotor consequent pole permanent magnet machine with H-type modular stator. *IEEE Access*, 9, pp.125331-125341.
- [13] Lee, C.H., Chau, K.T. and Liu, C., 2015. Design and analysis of a cost-effective magnet less multiphase flux-reversal DC-field machine for wind power generation. *IEEE Transactions on Energy Conversion*, 30(4), pp.1565-1573.
- [14] Z. Q. Zhu, Y. Pang, D. Howe, S. Iwasaki, R. Deodhar, and A. Pride, "Analysis of electromagnetic performance of flux-switching permanent-magnet machines by nonlinear adaptive lumped parameter magnetic circuit model," *IEEE Trans. Magn.*, vol. 41, no. 11, Nov. 2005.
- [15] R. L. Owen, Z. Q. Zhu, and G. W. Jewell, "Hybrid excited flux-switching permanent magnet machines with iron flux bridges," *IEEE Trans. Magn.*, vol. 46, no. 6, pp. 1726–1729, Jun. 2010.
- [16] J. T. Chen, Z. Q. Zhu, S. Iwasaki, and R. Deodhar, "A novel hybrid excited flux-switching brushless ac machines for EV/HEV applications," in *Proc. IEEE VPPC*, 2010, pp. 1–6.
- [17] Y. Tang, T. E. Motosca, J. J. H. Paulides, and E. Lomonova, "Investigation of winding topologies for flux-switching machines," in *Proc. 15th Int. Symp. Electromagn. Fields in Mechatron., Electric. Electron. Eng., Funchal, Madeira, Sep. 2011*, pp. 1–8.
- [18] E. Ilhan, T. E. Motosca, J. J. H. Paulides, and E. Lomonova, "Energy conversion loops for flux-switching PM machine analysis," in *Proc. 15th Int. Symp. Electromagn. Fields in Mechatron., Electric. Electron. Eng., Funchal, Madeira, Sep. 2011*, pp. 1–8.
- [19] D. S. More, H. Kalluru, and B. G. Fernandes, "Outer rotor flux reversal machine for rooftop wind generator," in *Proc. Ind. Appl. Soc. Annu. Meeting, Edmonton, AB, Canada, 2008*, pp. 1-6.
- [20] Zulu, B. C. Mecrow and M. Armstrong, "A Wound-Field Three-Phase Flux-Switching

Synchronous Motor with All Excitation Sources on the Stator," in IEEE Transactions on Industry Applications, vol. 46, no. 6, pp. 2363-2371, Nov.-Dec. 2010, doi: 10.1109/TIA.2010.2072972.